

Original Article

IL-13 alleviates idiopathic pulmonary hypertension by inhibiting the proliferation of pulmonary artery smooth muscle cells and regulating macrophage infiltration

Ruda Wei^{1*}, Liting Chen^{1,2*}, Pengchuan Li^{1*}, Chaoyang Lin³, Qingshi Zeng⁴

¹Hebei North University, Zhangjiakou 075000, Hebei, P. R. China; ²Department of Cardiovascular Medicine, Air force Medical Center, PLA, Beijing 100142, P. R. China; ³Department of Internal Medicine, Dachong Hospital of Zhongshan, Zhongshan 528476, Guangdong, P. R. China; ⁴Department of Radiology, The First Affiliated Hospital of Shandong First Medical University & Shandong Provincial Qianfoshan Hospital, Jinan 250011, Shandong, P. R. China. *Equal contributors.

Received January 19, 2022; Accepted May 18, 2022; Epub July 15, 2022; Published July 30, 2022

Abstract: Background: Idiopathic pulmonary arterial hypertension (IPAH) is characterized by medial hypertrophy due to pulmonary artery smooth muscle cell (PASMC) hyperplasia. In the present study, we conducted bioinformatic analyses and cellular experiments to assess the involvement of the interleukin-13 (IL-13) in IPAH. Methods: The differentially expressed genes (DEGs) in IPAH and DEGs in IPAH caused by IL-13 treatment were screened using the GEO database. PPI networks were used to analyze the hub genes. Hypoxia-induced PSMCs were treated with IL-13 for *in vitro* assays. CCK8 and EdU staining were used to observe proliferation of PSMCs, and RT-qPCR was applied to detect the expression of hub genes. The conserved binding sites of microRNAs (miRNAs) in the 3'UTR of hub genes were investigated, and the regulatory relationships of the relevant miRNAs on their targets were verified by RT-qPCR and dual-luciferase assays. The GO and KEGG analyses were performed to study the downstream pathways. The effect of hub genes on immune cell infiltration in IPAH was investigated. Results: IL-13 altered gene expression in IPAH. IL-13 inhibited the proliferation and the expression of hub genes in PSMCs. The 3'UTR sites between HNRNPA2B1, HNRNPH1, SRSF1, HNRNPU and HNRNPA3 in the hub genes and candidate regulatory miRNAs were well conserved in humans. IL-13-mediated hub genes regulated multiple pathways and influenced immune cell infiltration. Hypoxia-induced PSMCs promoted the M2 polarization of macrophages, whereas IL-13-treated PSMCs skewed the macrophages toward M1 polarization. Conclusions: IL-13-mediated alterations in hub genes inhibit PASM proliferation and promote M1 macrophage infiltration in IPAH.

Keywords: Idiopathic pulmonary arterial hypertension, IL-13, pulmonary artery smooth muscle cells, bioinformatics analysis, macrophage

Introduction

Idiopathic pulmonary arterial hypertension (IPAH) is a cardiopulmonary vascular disease with unknown etiology and a very high fatality rate. According to estimates by the ESC/ERS, the annual number of adults newly diagnosed with IPAH worldwide is approximately 5.9 per million [1, 2]. The main clinical manifestations of IPAH are a gradual increase in pulmonary artery pressure, right ventricular hypertrophy, and right heart failure [3]. Pathological manifestations include excessive pulmonary vasoconstriction, migration and proliferation of pul-

monary arterial smooth muscle cells (PASECs), and endothelial cell fibrosis, resulting in pulmonary plexiform lesions, vascular occlusion, and in situ thrombosis [4].

Although the pathogenic mechanism of IPAH is still unknown, increasing evidence shows that immune inflammation plays a key role in the occurrence and development of IPAH [5]. The infiltration of inflammatory cells such as monocytes/macrophages, dendritic cells, T lymphocytes, and B lymphocytes is observed around the pulmonary plexiform lesions of IPAH patients, and the levels of pro-inflammatory fac-

IL-13 is involved in the progression of IPAH

tors in the peripheral blood of IPAH patients are abnormally increased [5-7], indicating that inflammatory cell infiltration is an important factor in IPAH pathogenesis. IL-13 is mainly secreted by Th2 cells and has 20-25% sequence homology with IL-4, which indicated that the immune function of IL-13 is similar to that of IL-4 [8]. It has been shown that IL-13 can inhibit the vasculitis response of IPAH by suppressing the proliferation of pulmonary artery smooth muscle cells (PASMCs) [9]. IL-13 forms a complex by chemotaxing low-affinity IL-13Ra1 and IL-4Ra, activating downstream signaling molecules to induce STAT3 and STAT6 signaling pathways, and inhibiting the migration and proliferation of PASECs as well as the secretion of endothelin-1 (ET-1) by endothelial cells [9]. On the other hand, it is involved in the vascular remodeling effect associated with IPAH due to its high-affinity binding to IL-13Ra2 [10]. However, the molecular mechanism of IL-13 in immune regulation during IPAH is still unclear.

Bioinformatics analyses and microarrays have been applied to clarify the pathogenic mechanism of various diseases and discover therapeutic targets in recent years. Therefore, in this study, two datasets from the Gene Expression Omnibus (GEO) database (<https://www.ncbi.nlm.nih.gov/geo>) were applied for bioinformatics analyses to identify differentially expressed genes (DEGs) and hub genes in IPAH patients stimulated by IL-13. Since current IPAH therapies are not curative and therapeutic approaches mostly target endothelial dysfunction [11], PASMC was used as a cell model for *in vitro* assays to understand the molecular mechanism of IL-13 in immune regulation of IPAH.

Material and methods

Dataset acquisition

The microarrays used in this study were obtained from the GEO database [12]. GSE15739 [9] dataset was analyzed using the GPL1708 platform (Agilent-012391 Whole Human Genome Oligo Microarray G4112A [Feature Number version]), including comparison of stimulated and unstimulated PASMCs (3 biological replicates, 2 time points). GSE130391 [13] dataset was analyzed using the GPL570 platform ([HG-U133_Plus_2] Affymetrix Human Genome U133 Plus 2.0 Array), including the pulmonary

artery tissues of 4 IPAH patients and 4 healthy controls.

Screening of differentially expressed genes

The online analysis tool GEO2R (www.ncbi.nlm.nih.gov/geo/geo2r/) was used to screen out the DEGs in GSE15739 dataset and GSE130391 dataset using the adjusted *P*-value (*adj. P*) <0.05, $|\log_2\text{fold change}| >1$ as the threshold.

Screening of co-expressed DEGs

OriginPro 2018 software was used to generate the volcano map. According to the order of the value of $|\log_2\text{fold change}|$, the top 60 DEGs were selected from the GSE15739 dataset and GSE130391 dataset, respectively. All of the co-expressed DEGs in the GSE15739 dataset and GSE130391 dataset and the co-expressed upregulated and downregulated DEGs were screened out by plotting Venn diagrams.

Co-expression of the DEG-encoded protein-protein interaction (PPI) network

The STRING 11.5 database (<https://cn.string-db.org/>) [14] was used to predict the global PPI network between the proteins encoded by DEGs co-expressed in GSE15739 dataset and GSE130391 dataset. The species was limited to "Homo sapiens", and the smallest combination core was 0.4. The global PPI network was visualized with Cytoscape 3.7.1 software [15], and the CytoHubba plug-in was used to screen out the top 10 hub genes in the global PPI network.

Cell culture and treatment

The pulmonary arterial smooth muscle cell (PASMC, BFN60804009) was purchased from BLUEFBIO (Shanghai, China). The cells were cultured with high-glucose DMEM supplemented with 10% fetal bovine serum and 1% penicillin/streptomycin and maintained at 37°C in 5% CO₂. Human macrophages (CP-H186) were purchased from Procell (Wuhan, Hubei, China) and cultured at 37°C in 5% CO₂ using Procell's special growth culture medium. Referring to a previous report [16], PASMCs were cultured under hypoxia (1% O₂) for 48 h to construct an *in vitro* model of IPAH, and cells cultured in normoxia (21% O₂) served as a control. PASMCs were stimulated with or without IL-13 (10 ng/ml) for

IL-13 is involved in the progression of IPAH

6 h during hypoxic culture. The treated PASMCMedium was collected and used as a conditioned medium to treat macrophages for 24 h. The microRNA (miRNA) mimic used for cell transfection and its control were purchased from Guangzhou RiboBio Co., Ltd. (Guangzhou, Guangdong, China), and all transfections were performed using Lipofectamin 2000 according to the manufacturer's protocol.

Cell counting kit-8 (CCK-8)

CCK-8 (Beyotime Biotechnology Co., Ltd., Shanghai, China) was used to assay PASMCM viability. PASMCMs were seeded at 2000 cells/well into 96-well plates and treated with hypoxia induction and/or IL-13. Subsequently, 10 μ L CCK-8 solution was added to each well, and incubation was continued for 2 h. Cell viability was measured by determining the optical density (OD) value at 450 nm using a microplate reader.

EdU assay

Cell-Light EdU Apollo643 In Vitro Kit (RiboBio) was used to detect DNA synthesis in cells. PASMCMs were seeded at 1×10^5 cells/well into 96-well plates, followed by hypoxia induction and/or IL-13 treatment. Subsequently, the cells were incubated with 100 μ L of 50 μ M EdU for 2 h, fixed with PBS containing 4% paraformaldehyde for 30 min at room temperature, and permeabilized with PBS containing 0.5% TritonX-100 for 10 min. The cells were stained with 1 \times Apollo[®] Staining Reaction Solution for 30 min at room temperature in the dark, followed by 1 \times Hoechst 33342 for 30 minutes at room temperature in the dark for nuclei-counterstaining. Images were acquired by confocal fluorescence microscopy (Carl Zeiss, Oberkochen, Germany) for quantitative analysis of EdU-positive (red) cells.

Prediction of miRNAs of the top 10 hub target genes

The TargetScanHuman 8.0 database (http://www.targetscan.org/vert_80/) [17] was used to predict the regulatory miRNAs of the top 10 hub genes and the top five candidate miRNAs with the highest comprehensive scores. Moreover, the conserved 3'-untranslated region (3'UTR) in humans was predicted.

RNA isolation and RT-qPCR

Total RNA was extracted from the cells using TRIzol[™] reagent (Thermo Fisher Scientific Inc., Waltham, MA, USA). The extracted total RNA was reverse transcribed into cDNA using the First Strand cDNA Synthesis Kit (OriGene Technologies, Beijing, China) and qPCR was performed on ABI 7900HT using SensiMix SYBR Master Mix (OriGene). The relative gene expression was calculated using the $2^{-\Delta\Delta Ct}$ method. The housekeeping genes encoding β -actin and 5S were used as the internal reaction controls. The primer sequences used in this study are listed in **Table 1**.

Dual-luciferase assay

Binding sites for miRNAs on the 3'UTR of the hub genes were obtained from the TargetScanHuman 8.0 database. The wild type (WT)/mutant (MT) luciferase reporter plasmids of the corresponding hub genes were constructed by inserting the 3'UTR sequence containing the site or the site mutated into the pmiR-RB-Report[™] vector (RiboBio). The above plasmids were co-transfected into PASMCMs by Lipofectamin 2000 with mimic or NC mimic of the corresponding bound miRNAs, respectively. Luciferase activity was measured by Dual-Luciferase[®] Reporter Assay System (Promega Corporation, Madison, WI, USA) after 48 h.

Gene Ontology (GO) and Kyoto Encyclopedia of Genes and Genomes (KEGG) pathway enrichment analysis

The DAVID 6.8 database (<https://david.ncifcrf.gov/>) [18] was used to carry out the GO [18] and KEGG [14] enrichment analysis of the biological function of the total co-expressed DEGs, the upregulated and downregulated co-expressed DEGs, and the top 10 hub genes in GSE15739 dataset and GSE130391 dataset. $P < 0.05$ was considered statistically significant, and R language 4.0.3 software was used to visualize the results.

The expression of top 10 hub gene transcript mRNA and coding protein in normal lung tissue and the enrichment analysis of transcript mRNA in lung tissues and lung immune cells

The Human Protein Atlas 21.0 database (<https://www.proteinatlas.org/>) [19] was used

IL-13 is involved in the progression of IPAH

Table 1. Primers used in this study

Gene symbol	Forward primer (5'-3')	Reverse primer (5'-3')
HNRNPH1	TCCAGAGCACAAACAGGACACTG	GCTTACCAGTTACTCTGCCATC
EWSR1	AAAGGCGATGCCACAGTGTCT	TCATTGGAGGCTTCTCCGAGC
HNRNPA3	TTATGGGTCGCGGAGGGAACCT	CTCCTCCATAACTACCTCTGCTG
U2AFBP	GAACGTCTGTGACAACCTGGGA	AGGCTTCTCTGAAGTCCGTCAC
SNRPB	TTGGCACCTCAAGGCTTTTGAC	AGACCGAGGACTCGCTTCTCT
HNRNPU	GAGATTGCTGCCCGAAAGAAGC	TTCGCTGGAAGCCTGCAAACAG
SRSF1	TATCCGCGACATCGACCTCAAG	AAACTCCACCCGACAGCGGTAC
HNRNPA2B1	CAGCAACCTTCTAACTACGGTCC	CACTGCCTCTGGACCATAGTT
TARDBP	GATGGACGATGGTGTGACTGCA	AAGAACTCCCGCAGCTCATCCT
HNRNPA1	GCCCTGTCAAAGCAAGAGATGG	CGACCACTGAAGTTTCTCCAC
β-actin	CACCATTGGCAATGAGCGGTTT	AGGTCTTTGCGGATGTCCACGT
miR-490-3p	CATGGATCTCCAGTGTTG	GAACATGTCTGCGTATCTC
miR-383-5p	TCAGAAGGTGATTGTGGC	GAACATGTCTGCGTATCTC
miR-101-3p	CAGTTATCACAGTGCTGA	GAACATGTCTGCGTATCTC
miR-125-5p	CCTGAGACCCTTAAACC	GAACATGTCTGCGTATCTC
miR-10-5p	CCTGTAGATCCGAATTTG	GAACATGTCTGCGTATCTC
miR-1-3p	TGGAATGTAAAGAAGTATGT	GAACATGTCTGCGTATCTC
miR-206	GAATGTAAGGAAGTGTGTG	GAACATGTCTGCGTATCTC
miR-99-5p	AACCCGTAGATCCGATC	GAACATGTCTGCGTATCTC
miR-100-5p	CCGTAGATCCGAACCTTG	GAACATGTCTGCGTATCTC
miR-155-5p	TGCTAATCGTGATAGGGG	GAACATGTCTGCGTATCTC
5S	CTCGCTTCGGCAGCACAT	TTTGCCTGTCATCCTTGCG
CXCL12	CTCAACTCCAAACTGTGCC	CTCCAGGTACTCCTGAATCCAC
ARG1	TCATCTGGGTGGATGCTCACAC	GAGAATCCTGGCACATCGGGAA
iNOS	GCTCTACACCTCCAATGTGACC	CTGCCGAGATTTGAGCCTCATG
TNF-α	CTCTTCTGCCTGCTGCACTTTG	ATGGGCTACAGGCTTGTCACTC

Note: HNRNPH1, heterogeneous nuclear ribonucleoprotein H1; EWSR1, Ewing Saroma Breakpoint Region 1; HNRNPA3, heterogeneous nuclear ribonucleoprotein A3; U2AFBP, U2 small nuclear RNA auxiliary factor BP; SNRPB, small nuclear ribonucleoprotein polypeptides B; HNRNPU, heterogeneous nuclear ribonucleoprotein U; SRSF1, serine splicing factor 1; HNRNPA2B1, heterogeneous nuclear ribonucleoprotein A2B1; TARDBP, TAR DNAbinding protein 43; HNRNPA1, heterogeneous nuclear ribonucleoprotein A1; miR, microRNA; CXCL12, C-X-C motif chemokine 12; ARG1, arginase-1; iNOS, inducible nitric oxide synthase; TNF, tumor necrosis factor.

to analyze the expression of top 10 hub gene transcript mRNA and coding protein in normal lung tissues and for transcript mRNAs in the enrichment analysis of lung tissues and lung immune cells.

Immune infiltration analysis of 22 types of immune cells in the lung tissues of IPAH patients

The CIBERSORTx database (<https://cibersortx.stanford.edu/>) [20] deconvolution algorithm was used to analyze the immune infiltration of immune cells into the pulmonary artery tissues in the GSE15739 dataset, IPAH patients and healthy controls from the GSE130391 dataset,

and the results were visualized using R language 4.0.3 software.

Statistical analysis

The data are expressed as mean ± SD. The results were obtained from at least three biological replicates. To determine the statistical significance, one-way or two-way analysis of variance (ANOVA) followed by a Tukey post hoc test for multiple comparisons were used. Statistical analysis and data visualization were performed with GraphPad Prism 8.0 software (GraphPad Software, San Diego, CA, USA). A *P*-value of less than 0.05 was considered statistically significant.

Results

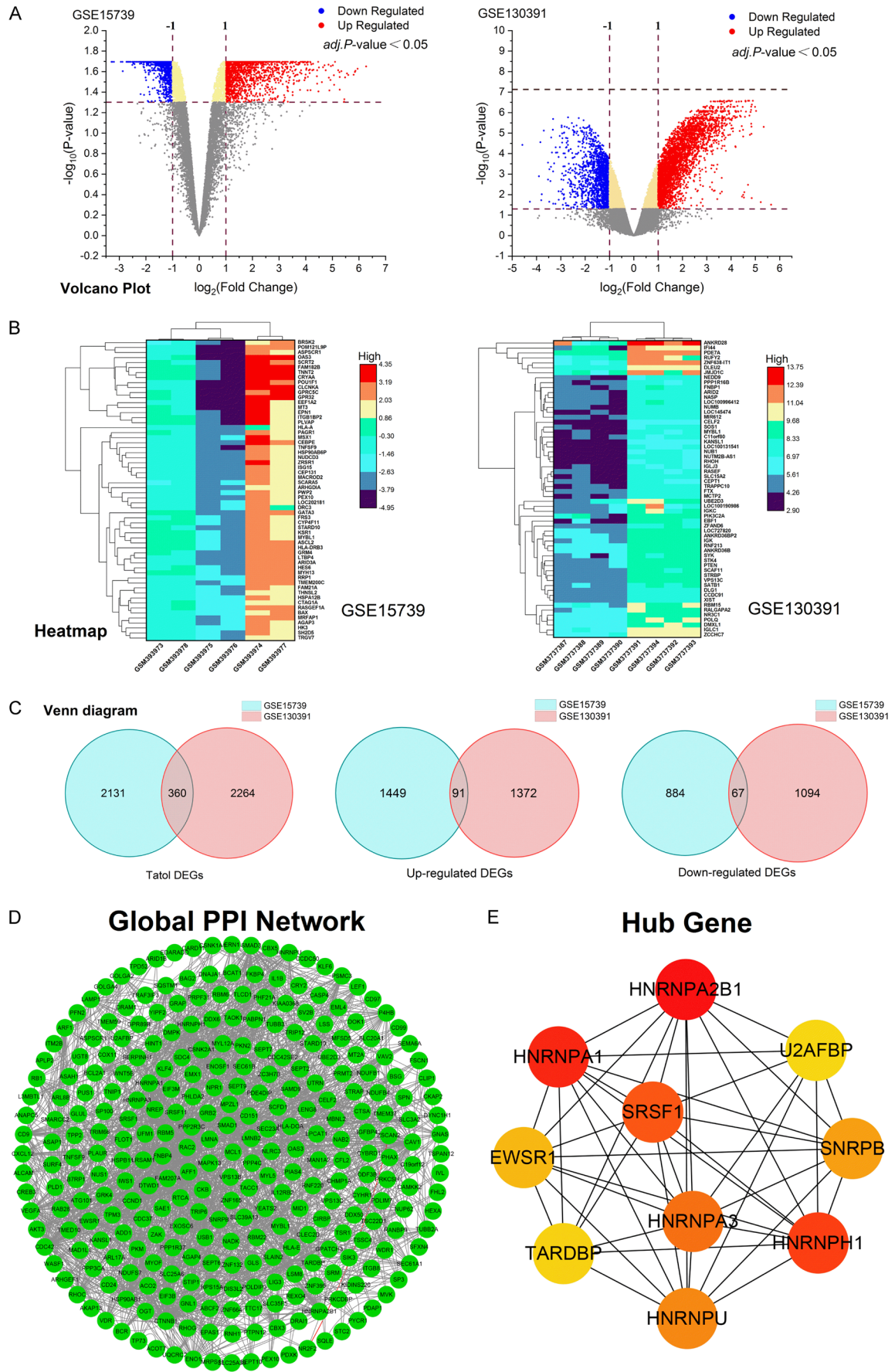
IL-13 treatment affects gene expression in IPAH

The datasets GSE130391 and GSE15739 were selected in the GEO database to screen for DEGs in IPAH and the effect of IL-13 treatment on gene expression in IPAH, respectively (**Figure 1A**). The cluster analysis showed that there were significant differences between the top 60

DEGs in the GSE15739 dataset and the GSE130391 dataset, indicating that IL-13 treatment leads to altered gene patterns in IPAH patients (**Figure 1B**). There was a total of 360 DEGs co-expressed in the GSE15739 dataset and GSE130391 dataset, of which 91 were upregulated and 67 were downregulated (**Figure 1C**).

The STRING 11.5 database was used to analyze the PPI networks off 360 co-expressed DEGs (**Figure 1D**). In addition, through the Cytoscape 3.7.1 software, the top 10 hub genes were selected from the PPI network, which were heterogeneous nuclear ribonucleoprotein

IL-13 is involved in the progression of IPAH



IL-13 is involved in the progression of IPAH

Figure 1. IL-13 regulates the expression of genes in IPAH. A. Volcano maps of DEGs in the GSE15739 and GSE130391 datasets screened with $\text{adj. } P < 0.05$ and $|\log_2\text{Fold Change}| > 1$. B. Top 60 DEGs in the GSE15739 and GSE130391 datasets, respectively. C. Intersecting genes in the DEGs of the two datasets. D. PPI network analysis of 360 DEGs. E. The top 10 hub genes in the PPI network.

A2B1 (HNRNPA2B1), heterogeneous nuclear ribonucleoprotein A1 (HNRNPA1), Ewing Sarcoma Breakpoint Region 1 (EWSR1), TAR DNA-binding protein 43 (TARDBP), heterogeneous nuclear ribonucleoprotein U (HNRNPU), heterogeneous nuclear ribonucleoprotein H1 (HNRNPH1), small nuclear ribonucleoprotein polypeptides B (SNRPB), U2 small nuclear RNA auxiliary factor BP (U2AFBP), serine splicing factor 1 (SRSF1), and heterogeneous nuclear ribonucleoprotein A3 (HNRNPA3) (**Figure 1E**). IL-13-induced changes in the expression of most of these 10 hub genes differed from those caused by IPAH. Only SRSF1, HNRNPA2B1, TARDBP, and HNRNPA1 expression was significantly elevated in IPAH patients as well as in IL-13-treated PSMCs. HNRNPH1, EWSR1, and HNRNPA3 expression was downregulated after IL-13 stimulation and upregulated in IPAH patients. U2AFBP, SNRPB, and HNRNPU expression was downregulated in IPAH patients, while IL-13 treatment promoted their expression.

IL-13 regulates hypoxia-induced changes in PSMC proliferation and hub gene expression

We constructed an *in vitro* model of IPAH by hypoxia treatment, followed by IL-13 treatment. Analyzing changes in cell viability by CCK8, we observed that IL-13 treatment inhibited hypoxia-induced cell proliferation (**Figure 2A**). In contrast, EdU staining results showed a hypoxia-induced increase in cellular DNA synthesis, which was inhibited by IL-13 treatment (**Figure 2B**). By RT-qPCR we examined the effect of hypoxia induction and IL-13 treatment on hub gene expression in PSMCs (**Figure 2C**). Hypoxia elevated expression of HNRNPH1, EWSR1, HNRNPA3 and downregulated expression of U2AFBP, SNRPB, and HNRNPU in PSMCs. IL-13 treatment significantly attenuated hypoxia-induced gene expression changes. SRSF1, HNRNPA2B1, TARDBP, and HNRNPA1 all exhibited elevated expression upon hypoxia and IL-13 treatment.

Analysis of conserved binding sites of hub genes

Through the TargetScanHuman 8.0 database reverse prediction software, the top five closely

related posttranscriptional candidate regulatory miRNAs were screened out according to the comprehensive score of the top 10 hub target genes and the conservation of the 3'UTR position in humans. The highest comprehensive scores represented the most closely related miRNAs (**Table 2**). The mimic of the relevant miRNAs was transfected and the expression of the corresponding genes and miRNAs in the cells was detected by RT-qPCR (**Figure 3A**). The binding relations between miR-490-3p and HNRNPA2B1, miR-383-5p and HNRNPH1, miR-10-5p and SRSF1, miR-1-3p/206 and HNRNPU, miR-155-5p and HNRNPA3 were verified. Overexpression of the relevant miRNAs all led to downregulation of the expression of the corresponding target genes. We verified whether the 3'UTR of HNRNPA2B1, HNRNPH1, SRSF1, HNRNPU and HNRNPA3 was regulated by the most closely related miRNAs by dual-luciferase assays (**Figure 3B**). The 3'UTR sites of the HNRNPA2B1, HNRNPH1, SRSF1, HNRNPU, and HNRNPA3 by posttranscription candidate regulatory miRNAs are well conserved in humans.

GO enrichment analysis of co-expressed DEGs

GO enrichment analysis comprises biological process (BP), cellular component (CC), and molecular function (MF). In the context of IPAH, 360 co-expressed DEGs have a wide range of CC, mainly involved in the regulation of gene expression and molecular interactions in IPAH, and suggested to be associated with MF such as cell-cell adhesion (**Figure 4A**). GO enrichment analysis of upregulated co-expressed DEGs (**Figure 4B**), downregulated co-expressed DEGs (**Figure 4C**) and 10 hub genes (**Figure 4D**) alone demonstrated similar results. In a word, these DEGs are extensively involved in gene expression and molecular interactions in IPAH.

KEGG pathway enrichment analysis among co-expressed DEGs

The KEGG signaling pathway is a set of signaling pathways that reflect the knowledge of molecular interactions, reactions, and relationships. Screening was performed according to $P < 0.05$. There were 22 KEGG signaling pathways enriched among the co-expressed DEGs

IL-13 is involved in the progression of IPAH

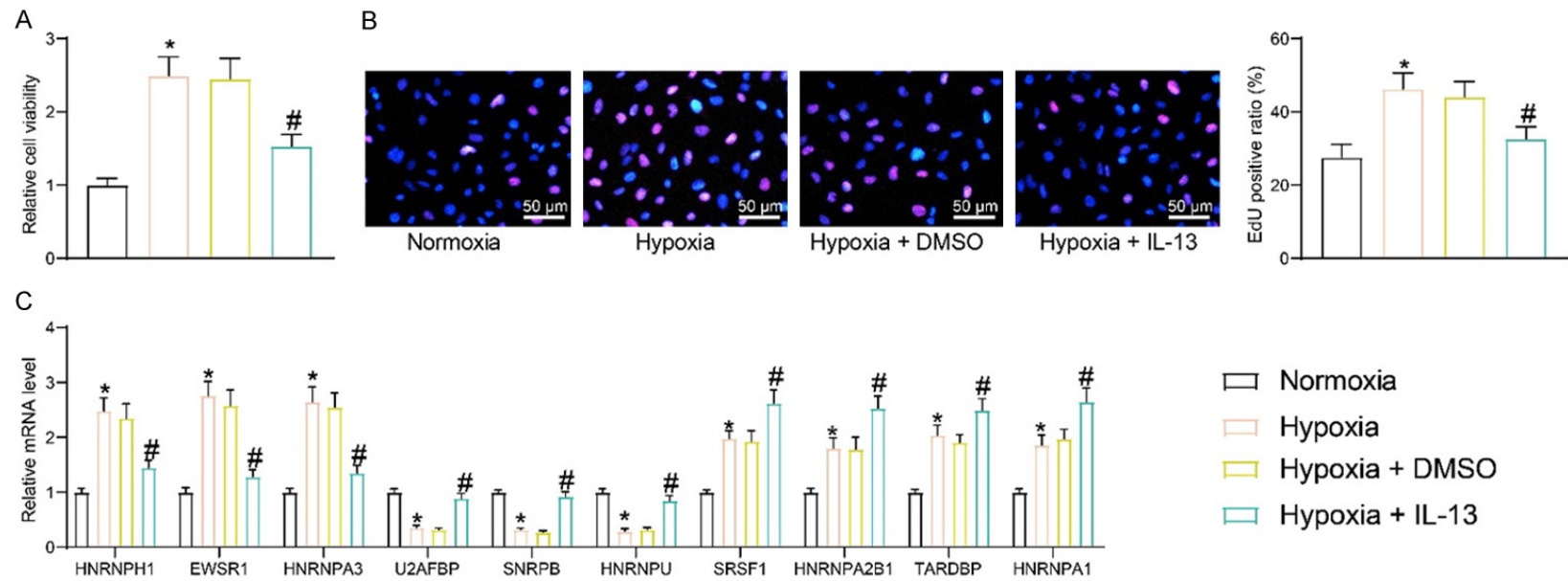


Figure 2. IL-13 inhibits hypoxia-induced changes in PASM cell proliferation and hub gene expression. A. The effect of hypoxia induction and IL-13 treatment on cell viability using CCK8. B. The effect of hypoxia induction and IL-13 treatment on cellular DNA synthesis using EdU staining. C. The effects of hypoxia induction and IL-13 treatment on mRNA expression in cells using RT-qPCR. Values represent the mean \pm SD; *P<0.01 versus normoxia, #P<0.01 versus hypoxia + DMSO. One-way or two-way ANOVA followed by a Tukey post hoc test for multiple comparisons was used.

IL-13 is involved in the progression of IPAH

Table 2. The comprehensive scores of posttranscriptional candidate regulatory miRNAs closely related to the top 10 hub target genes and the conservation of posttranscriptional regulatory 3'UTR sites in humans

Hub Gene	HNRNPA2B1	HNRNPH1	U2AFBP	EWSR1	SNRPB	SRSF1	HNRNPU	TARDBP	HNRNPA3	HNRNPA1
	miR-490-3p	miR-383-5p	-	miR-101-3p	miR-125-5p	miR-10-5p	miR-1-3p/206	miR-99-5p/100-5p	miR-155-5p	miR-27-3p
	miR-148-3p/152-3p	miR-200bc-3p/429-3p	-	-	-	miR-204-5p/211-5p	miR-122-5p	miR-142-3p	miR-221-3p/222-3p	miR-24-3p
miRNAs	miR-103-3p/107	miR-22-3p	-	-	-	miR-216b-5p	miR-155-5p	miR-802	miR-1-3p/206	miR-490-3p
	miR-302c-3p.2/520-3p	miR-132-3p/212-3p	-	-	-	miR-1-3p/206	miR-135-5p	miR-302-3p/372-3p/373-3p/520-3p	miR-802	miR-34-5p/449-5p
	miR-30-5p	miR-181-5p	-	-	-	miR-23-3p	miR-124-3p.1	miR-181-5p	miR-218-5p	miR-153-3p
	-0.77	-0.25	-	-0.16	-0.23	-0.75	-0.55	-0.56	-0.57	-0.64
	-0.46	-0.21	-	-	-	-0.58	-0.43	-0.47	-0.54	-0.58
Total context score	-0.44	-0.2	-	-	-	-0.49	-0.42	-0.4	-0.53	-0.54
	-0.32	-0.17	-	-	-	-0.48	-0.36	-0.34	-0.52	-0.45
	-0.32	-0.1	-	-	-	-0.47	-0.36	-0.3	-0.46	-0.32
	0.27	<0.1	-	0.21	<0.1	0.65	0.98	<0.1	0.44	<0.1
	<0.1	0.42	-	-	-	<0.1	0.55	0.74	0.13	0.35
Aggregate PCT	0.79	<0.1	-	-	-	<0.1	<0.1	<0.1	0.93	0.54
	0.42	0.25	-	-	-	0.84	0.77	0.24	0.55	0.31
	<0.1	<0.1	-	-	-	0.14	<0.1	0.71	0.39	<0.1
	75-81	130-136	-	N/A	N/A	431-437	86-93	N/A	697-704	N/A
	2425-2431	273-279	-	-	-	N/A	475-482	N/A	1243-1250	2433-2440
Conserved 3'UTR	719-725	22-28	-	-	-	17-23	N/A	538-545	256-262	55-61
	2012-2018	N/A	-	-	-	17-23	1421-1427	1860-1866	151-157	2455-2462
	2248-2255	112-118	-	-	-	N/A	N/A	453-459	1042-1049	593-600

Note: HNRNPH1, heterogeneous nuclear ribonucleoprotein H1; EWSR1, Ewing Saroma Breakpoint Region 1; HNRNPA3, heterogeneous nuclear ribonucleoprotein A3; U2AFBP, U2 small nuclear RNA auxiliary factor BP; SNRPB, small nuclear ribonucleoprotein polypeptides B; HNRNPU, heterogeneous nuclear ribonucleoprotein U; SRSF1, serine splicing factor 1; HNRNPA2B1, heterogeneous nuclear ribonucleoprotein A2B1; TARDBP, TAR DNA-binding protein 43; HNRNPA1, heterogeneous nuclear ribonucleoprotein A1; miR, microRNA; 3'UTR, 3' untranslated region; N/A, not applicable.

IL-13 is involved in the progression of IPAH

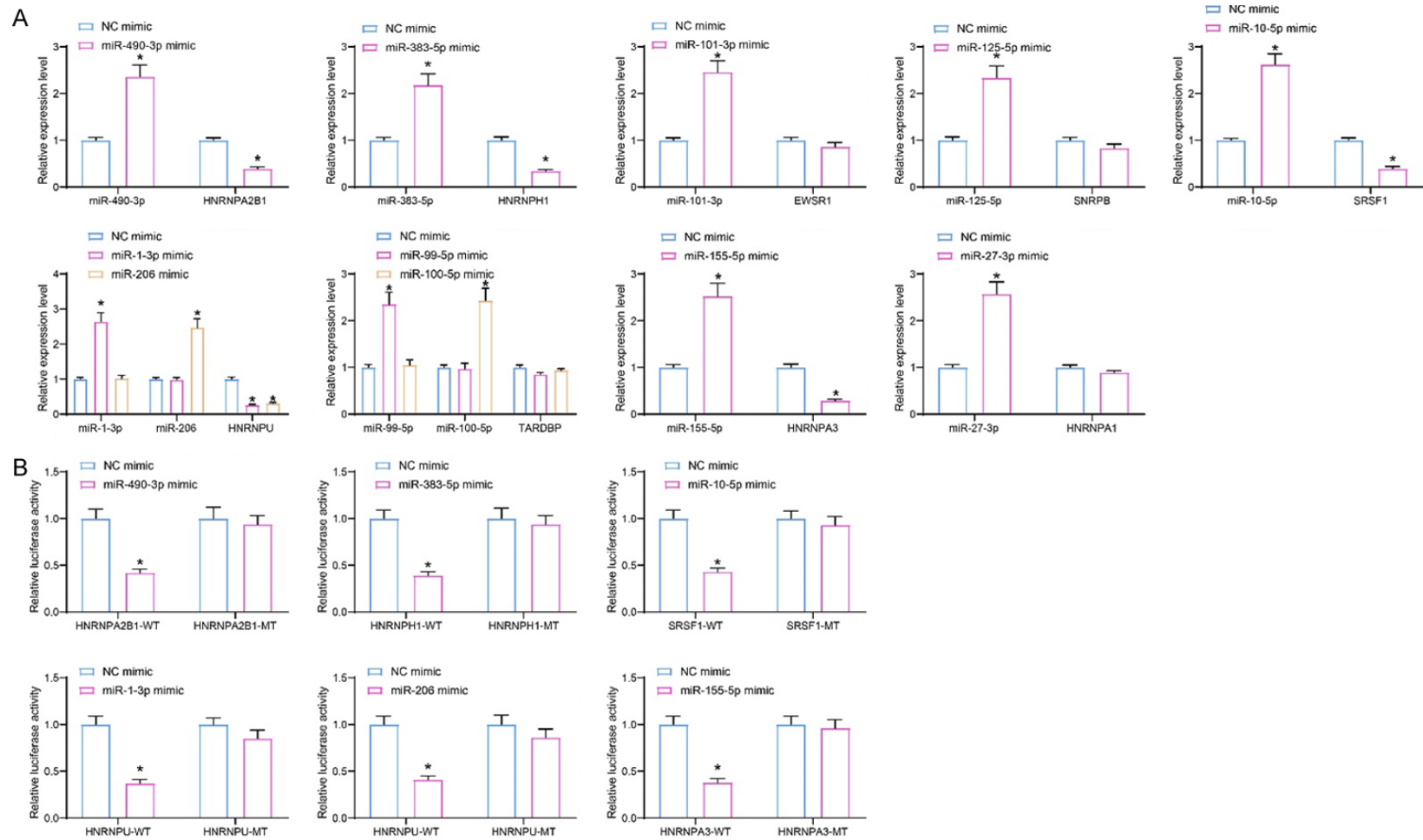
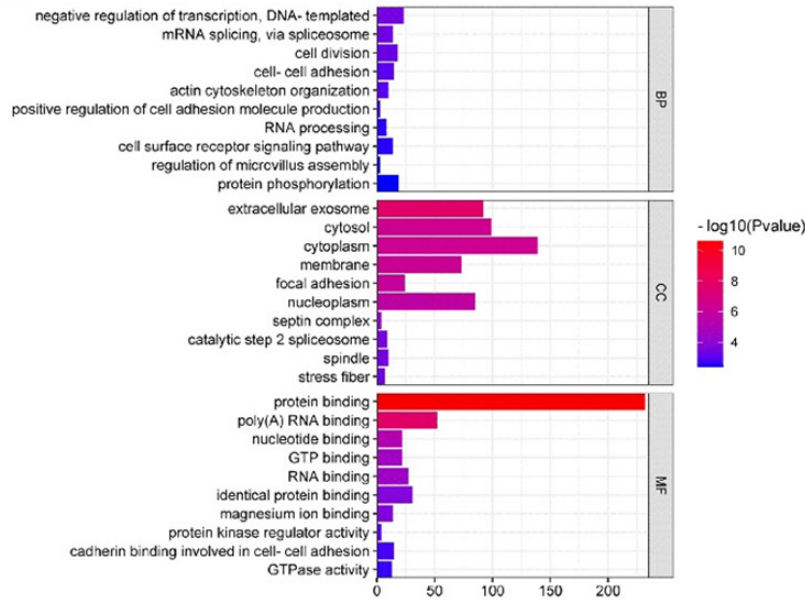


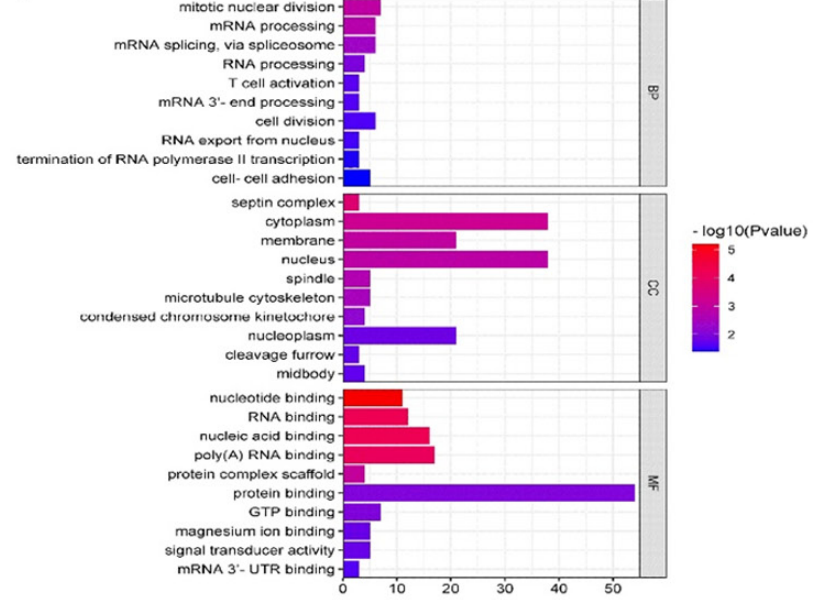
Figure 3. Analysis of bound miRNAs by 3'UTR sites of hub genes. A. The effect of miRNAs on the expression of their target genes using RT-qPCR. B. The binding of miRNAs to hub genes using dual-luciferase assay. Values represent the mean \pm SD; * $P < 0.01$ versus NC mimic. Two-way ANOVA followed by a Tukey post hoc test for multiple comparisons was used.

IL-13 is involved in the progression of IPAH

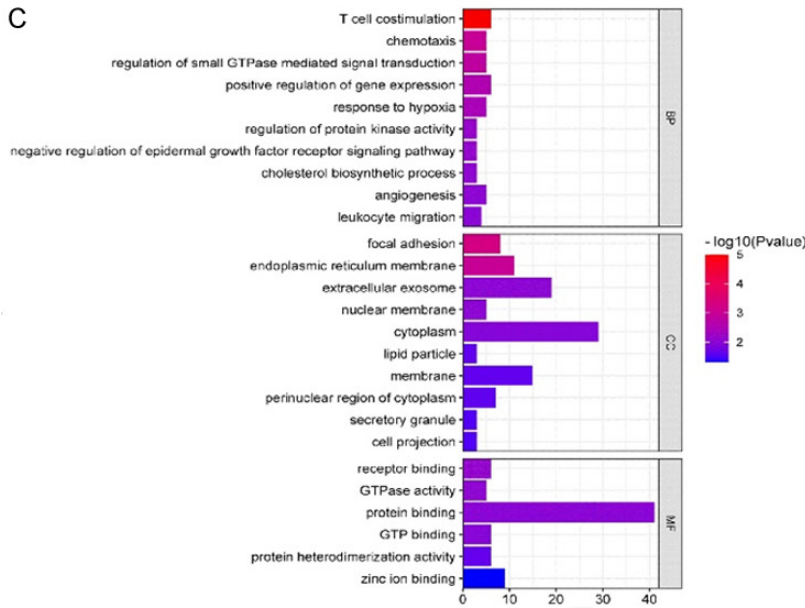
A



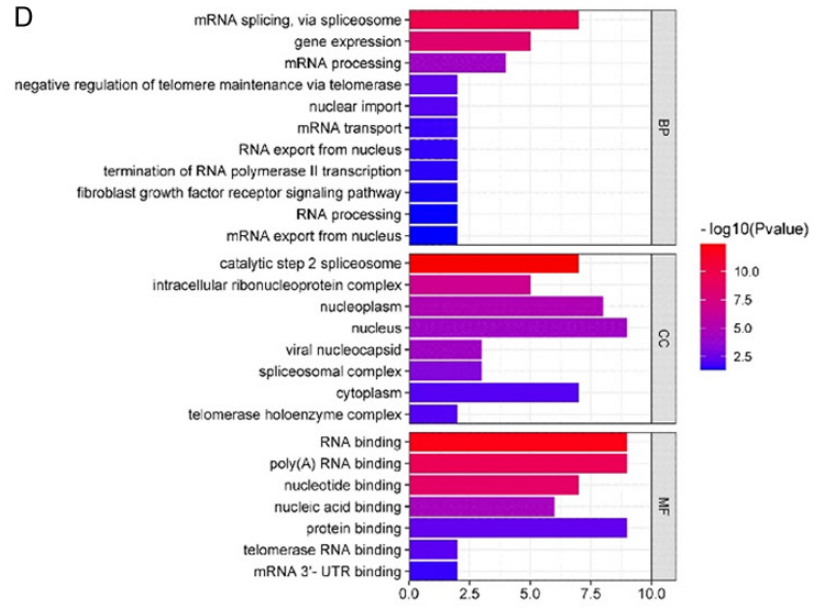
B



C



D



IL-13 is involved in the progression of IPAH

Figure 4. GO enrichment analysis of DEGs. A. GO enrichment analysis of co-expressed DEGs. B. GO enrichment analysis of upregulated co-expressed DEGs. C. GO enrichment analysis of downregulated co-expressed DEGs. D. GO enrichment analysis of top 10 hub genes.

(**Figure 5A**). The most significant KEGG signaling pathway involved was bacterial invasion of epithelial cells (**Figure 5B**), suggesting that these DEGs were associated with immune responses. There were 11 KEGG signaling pathways enrichment in the downregulated co-expressed DEGs (**Figure 5C**). The most significant KEGG signaling pathway was focal adhesion (**Figure 5D**). However, the KEGG signaling pathway analysis of the top 10 hub genes revealed enrichment only in spliceosome. The upregulated co-expressed DEGs were not significantly enriched in any KEGG signaling pathways.

The analysis of single-cell expression of hub genes and IL-13-mediated immune responses

The Human Protein Atlas 21.0 database was used to analyze the expression of top 10 hub genes in different types of cells (**Table 3**). The top 10 hub gene transcript mRNAs were usually enriched in endothelial cells, smooth muscle cells and fibroblasts, with some variation in gene expression in different cells. Hub gene expression exhibited some cellular specificity in immune cells. HNRNPA2B1, HNRNPH1, SRSF1, HNRNPU, TARDBP and HNRNPA3 expression was higher in NK cells. HNRNPH1, SRSF1, HNRNPU, TARDBP and HNRNPA3 gene expression was higher in B lymphocytes, while HNRNPH1 was highly expressed in T lymphocytes. SNRPB and HNRNPA3 expression was higher in neutrophils, and HNRNPA2B1, HNRNPH1, SRSF1, HNRNPU, TARDBP, HNRNPA3 and HNRNPA1 gene expression was higher in mast cells. The transcripts of macrophages and plasma cells were not significantly enriched in mRNAs.

We analyzed the immune infiltration of 22 types of immune cells into the pulmonary artery tissues in the GSE15739 dataset and the GSE130391 dataset through the CIBERSORTx database. According to the abundance of immune infiltration of immune cells in pulmonary artery tissues (**Figure 6A**), IPAH, as well as IL13 stimulation, resulted in altered immune infiltration abundance of immune cells. The correlation heatmap of the 22 types of immune cells

(**Figure 6B**) showed that after IL-13 stimulation, the correlation between the proinflammatory immune cells in the pulmonary artery tissue of IPAH patients decreased. Subsequently, the degree of infiltration of individual immune cells stimulated by IPAH and IL-13 was compared (**Figure 6C**). The numbers of $\gamma\delta$ T cells and M2 macrophages in the IPAH patients were higher than those in the healthy controls, while the numbers of activated dendritic cells in the healthy controls were higher than those in the IPAH patients. After IL-13 stimulation, un-activated memory CD4⁺T cells were inhibited, while M1 macrophages were promoted. This suggested that IL-13 significantly reversed the activation of M2 macrophages in IPAH, resulting in increased infiltration of M1 macrophages in lung tissues. The hypoxic environment in IPAH induces the production of M2 macrophages [21]. Therefore, the inhibitory effect of IL-13 on M2 macrophage activation demonstrates its potential therapeutic effect. Subsequently, we collected the culture medium of hypoxia- or IL-13-treated PSMCs as conditioned medium and used it for macrophage co-culture. The expression of M1/M2 polarization markers in macrophages was detected by RT-qPCR (**Figure 6D**). The results showed that hypoxia-induced PSMC-conditioned medium promoted expression of M2 macrophage markers (ARG1 and CXCL12) and decreased expression of M1 macrophage markers (iNOS and TNF- α), while IL-13 treatment significantly reversed hypoxia-induced changes in macrophage phenotype.

Discussion

There is still a lack of effective diagnostic and treatment methods for IPAH [22]. With the application of genome-wide association studies, it has been found that IPAH patients have mutations in pathogenic genes, which may promote the occurrence of IPAH and the development of right heart failure [23]. Moreover, various immune cells and effectors mediate DNA damage and promote apoptosis in PSMCs to induce pulmonary artery vascular remodeling [24]. Therefore, identifying the potential targets of IL-13 may reveal new strategies for the treatment of IPAH.

IL-13 is involved in the progression of IPAH

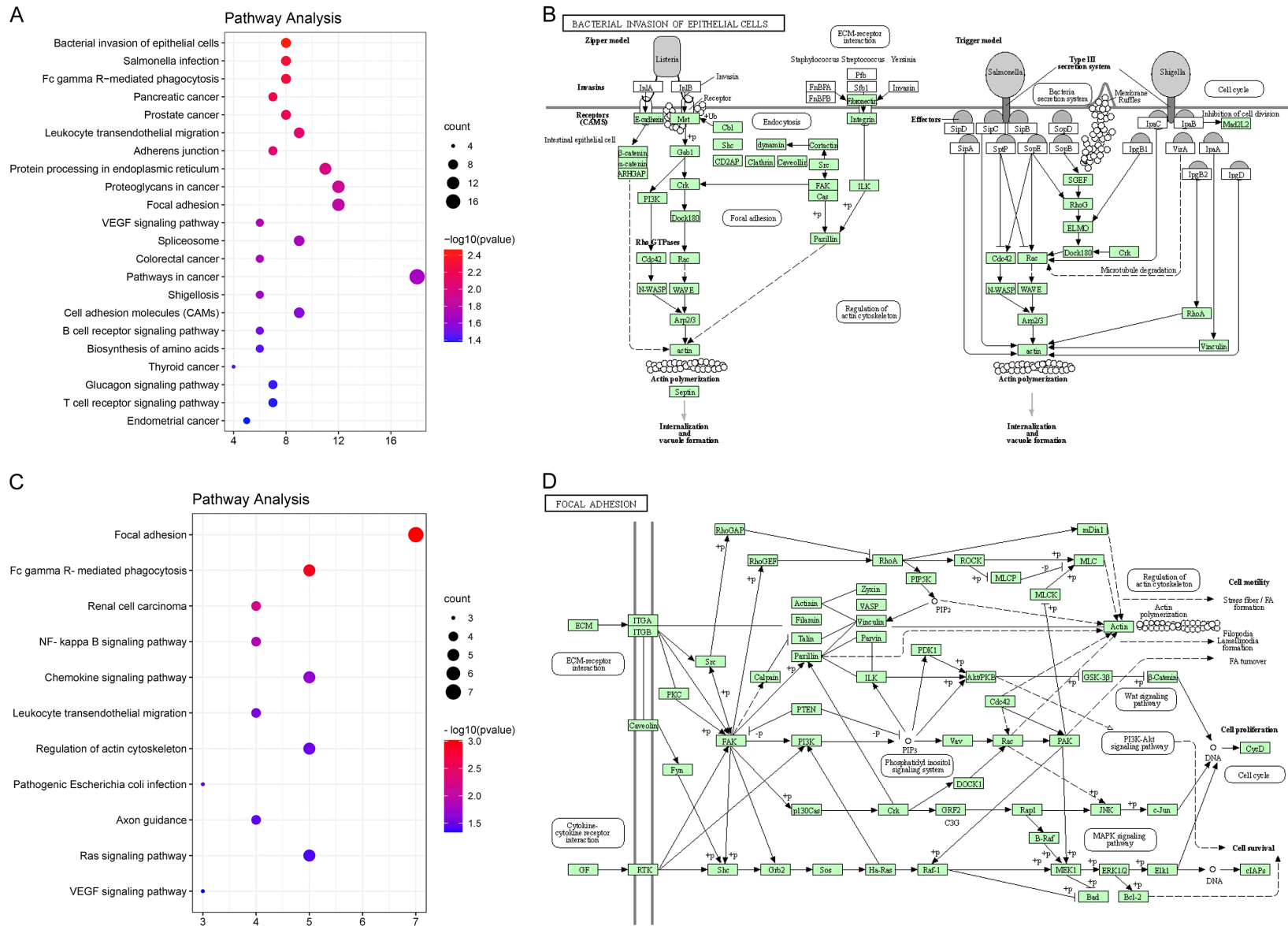


Figure 5. KEGG enrichment analysis of co-expressed DEGs. A. KEGG enrichment analysis of co-expressed DEGs. B. The bacterial invasion of epithelial cells signaling pathway. C. KEGG enrichment analysis of downregulated co-expressed DEGs. D. The focal adhesion signaling pathway.

IL-13 is involved in the progression of IPAH

Table 3. The expression level of the top 10 hub gene transcript mRNA and coding protein in normal lung tissues and the transcript mRNA enrichment analysis of lung tissue cells and immune cells in the lung

Hub Gene	HNRNPA2B1	HNRNPH1	U2AFBP	EWSR1	SNRPB	SRSF1	HNRNPU	TARDBP	HNRNPA3	HNRNPA1
Encoded Protein	Heterogeneous nuclear ribonucleoprotein A2/B1	Heterogeneous nuclear ribonucleoprotein H1	U2 small nuclear RNA auxiliary factor BP	EWS RNA binding protein 1	Small nuclear ribonucleoprotein B and B1	Serine and arginine rich splicing factor 1	Heterogeneous nuclear ribonucleoprotein U	TAR DNA binding protein	Heterogeneous nuclear ribonucleoprotein A3	Heterogeneous nuclear ribonucleoprotein A1
Expression of mRNA and Protein in lung tissue										
mRNA (Consensus dataset)	368.1 nTPM	103.4 nTPM	-	77.5 nTPM	112.6 nTPM	61.3 nTPM	81.4 nTPM	92.4 nTPM	176.7 nTPM	383.9 nTPM
Protein (Score)	Alveolar cells type I : High Alveolar cells type II: High Endothelial cells: High Macrophages : High	Alveolar cells: - Medium Macrophages: Medium	-	Alveolar cells type I : High Alveolar cells type II: High Endothelial cells: High Macrophages: High	Alveolar cells: High Macrophages: Medium	Alveolar cells type I : High Alveolar cells type II: Medium Endothelial cells: High	Alveolar cells type I : High Alveolar cells type II: High Endothelial cells: High Macrophages: High	Alveolar cells type I : High Alveolar cells type II: High Endothelial cells: High Macrophages: High	Alveolar cells: High Macrophages: Medium	Alveolar cells: High Macrophages: High
mRNA enrichment of lung tissue and immune cells										
Tissue cells										
Respiratory ciliated cells	0.056	0.110	-	0.045	-0.069	0.135	0.099	0.103	0.089	0.079
Alveolar cells type I	0.145	0.187	-	0.058	-0.009	0.042	0.170	0.230	0.097	-0.056
Alveolar cells type II	-0.401	-0.399	-	-0.073	-0.045	-0.552	-0.301	-0.408	-0.455	-0.327
Mitotic cells	-0.073	-0.209	-	0.001	-0.015	-0.162	-0.151	-0.142	-0.183	0.004
Endothelial cells	0.467	0.439	-	0.247	0.303	0.474	0.398	0.525	0.517	0.271
Smooth muscle cells	0.258	0.237	-	0.113	0.175	0.331	0.199	0.258	0.319	0.268
Fibroblast	0.383	0.421	-	0.127	0.034	0.460	0.391	0.430	0.453	0.295
Immune cells										
NK cells	0.475	0.473	-	0.156	0.098	0.520	0.451	0.470	0.505	0.210
B cells	0.189	0.326	-	-0.017	-0.029	0.321	0.220	0.221	0.286	0.172
T cells	0.176	0.305	-	0.069	-0.146	0.162	0.124	0.122	0.084	-0.011
Macrophages	-0.413	-0.490	-	-0.121	-0.128	-0.580	-0.461	-0.463	-0.584	-0.369
Neutrophils	0.075	0.079	-	-0.060	0.226	0.195	0.133	0.098	0.214	0.083
Mast cells	0.279	0.383	-	0.087	-0.032	0.310	0.290	0.321	0.314	0.203
Plasma cells	-0.132	-0.024	-	-0.033	-0.161	-0.135	-0.057	-0.133	-0.147	-0.108

Note: HNRNPH1, heterogeneous nuclear ribonucleoprotein H1; EWSR1, Ewing Sarcoma Breakpoint Region 1; HNRNPA3, heterogeneous nuclear ribonucleoprotein A3; U2AFBP, U2 small nuclear RNA auxiliary factor BP; SNRPB, small nuclear ribonucleoprotein polypeptides B; HNRNPU, heterogeneous nuclear ribonucleoprotein U; SRSF1, serine splicing factor 1; HNRNPA2B1, heterogeneous nuclear ribonucleoprotein A2B1; TARDBP, TAR DNA binding protein 43; HNRNPA1, heterogeneous nuclear ribonucleoprotein A1; TPM, transcript per million.

IL-13 is involved in the progression of IPAH

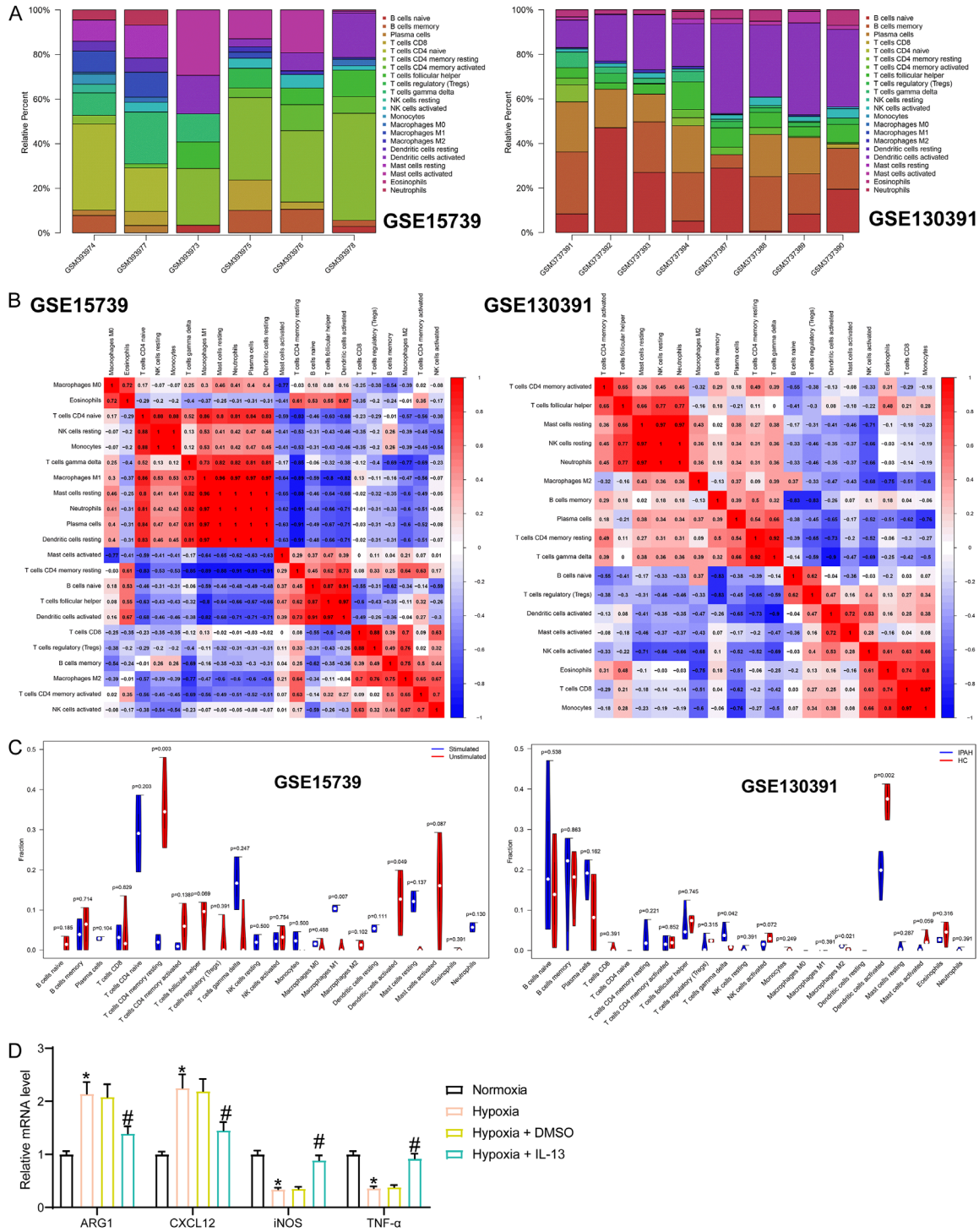


Figure 6. IL-13 mediates macrophage phenotypic changes in IPAH. **A.** The abundance of immune infiltration in the pulmonary artery tissue of 22 immune cells in the GSE15739 dataset and GSE130391 dataset. **B.** Correlation heatmap of 22 immune cells in the pulmonary artery tissues in the GSE15739 dataset and GSE130391 dataset (the red square in the figure represents a positive correlation, and the blue represents a negative correlation; the darker the color, the stronger the correlation). **C.** Immune infiltration analysis of 22 kinds of immune cells in pulmonary artery tissues in the GSE15739 dataset and the GSE130391 dataset. **D.** Detection of gene expression in macrophages cultured with PASMC conditioned medium by RT-qPCR. Values represent the mean \pm SD; * $P < 0.01$ versus normoxia, # $P < 0.01$ versus hypoxia + DMSO. Two-way ANOVA followed by a Tukey post hoc test for multiple comparisons was used.

IL-13 is involved in the progression of IPAH

In this study, we obtained gene expression data from GEO datasets. Through bioinformatics analysis, 360 co-expressed DEGs were found to be associated with both IPAH and IL-13 stimulation, of which 91 were upregulated and 67 were downregulated. By generating a PPI network analysis of the 360 co-expressed DEGs, we identified top 10 hub genes, which were NRNPA2B1, HNRNPA1, EWSR1, TARDBP, HNRNPU, HNRNPH1, SNRPB, U2AFBP, SRSF1 and HNRNPA3. As a pleiotropic Th2 immune factor, IL-13 not only mediates the occurrence of tissue inflammation but also regulates immune balance [25, 26]. In the present study, we found that the viability of PASMCM induced by hypoxia was suppressed by IL-13 treatment. In the datasets, the downregulated U2AFBP, SNRPB and HNRNPU expression was restored by IL-13, and the IPAH-induced EWSR1, HNRNPH1 and HNRNPA3 were downregulated by IL-13. The similar trends were also observed in our treated PASMCM, which verified the credibility of our prediction results.

We also predicted the candidate regulatory miRNAs of these 10 hub genes and the 3'UTR of the hub genes in humans using Target-ScanHuman 8.0 database. The binding relation between miR-490-3p and HNRNPA2B1, miR-383-5p and HNRNPH1, miR-10-5p and SRSF1, miR-1-3p/206 and HNRNPU, miR-155-5p and HNRNPA3 was predicted and verified in PASMCMs. As a kind of endogenous noncoding single-stranded small RNA, miRNAs regulate the biological function of target genes by binding to the 3'UTR site of mRNAs [27]. miR-101-3p inhibits the migration and proliferation of endothelial cells and fibrosis of the cardiovascular system, but the overexpression of miR-101-3p aggravates inflammation-mediated myocardial damage [27, 28]. miR-125-5p inhibits the expression of proinflammatory factors and cell apoptosis through the JAK1/STAT3 and NF- κ B signaling pathways [29]. miR-1-3p/206 can improve vascular damage in ischemic diseases [30], while miR-383-5p has the opposite regulatory effect, regulating cell apoptosis [31] and aggravating vascular damage in ischemic diseases [32]. miR-155-5p enhances the proinflammatory response and inhibits the immune effect of IL-13 by polarizing M1 macrophages and inhibiting their apoptosis, downregulating Th2 cells [33, 34]. However, miR-155-5p also inhibits the abnormal migration and prolifera-

tion of vascular smooth muscle cells and endothelial cells [35], which shows that miR-155-5p has a pleiotropic regulatory effect in the pathogenic mechanism of IPAH. Our results suggest that the posttranscriptional regulation of the hub genes by miRNAs is involved in the pathogenesis of IPAH. In addition, the 3'UTR target sites of miR-1-3p/206, miR-383-5p, and miR-155-5p are well conserved in humans and may become important candidate targets for the treatment of IPAH.

It is notable that four out of the ten hub genes belong to the HNRNP family which participates in alternative splicing, mRNA transcription, and posttranscriptional microRNA regulation [36]. It has been revealed that HNRNPA2B1 mediates the IFN- α/β through proinflammatory factors and the TBK1-IRF3 signaling pathway to enhance the antiviral immune response [37]. The HNRNPA1 and HNRNPU genes may be important targets for inducing immune inflammation in chronic respiratory diseases, such as COPD and bronchial asthma [38, 39]. HNRNPH1 is involved in the viral replication process [40]. EWSR1 and HNRNPA3 are involved in the regulation of cell apoptosis and other processes [41, 42]. TARDBP initiates the inflammatory response through the interaction of CD14 and Toll-like receptor 4 [43]. Immune imbalance mediated by TARDBP is involved in the pathogenesis of systemic lupus erythematosus, Crohn's disease and other autoimmune diseases [44]. SRSF1 promotes the differentiation and proliferation of T lymphocytes, endothelial cells and fibroblasts and promotes the proliferation of vascular smooth muscle through the D133p53-KLF5p21 pathway [45]. Thus, the existing reports were consistent with our prediction results that co-expressed DEGs and hub genes in IPAH patients participate in the regulation of cell signaling pathways and posttranscriptional regulation of mRNAs.

Our results further support that B cells, plasma cells, CD4⁺ T cells, Treg cells, and $\gamma\delta$ T cell numbers in IPAH patients are higher than those in healthy controls, while CD8⁺ T cell numbers are lower than in healthy controls. In the study of Xu J, et al. [46], the number of unactivated mast cells and M2 macrophages was higher in IPAH patients than in healthy controls, which was supported by our findings. Our dataset may have been affected by the small sample size.

IL-13 is involved in the progression of IPAH

Our prediction results also showed that the activity of B cells, CD4⁺ T cells, and M2 macrophages in the pulmonary artery tissue was inhibited by IL-13. RT-qPCR assessment of M1- and M2-phenotype macrophages in PASMC challenged with hypoxia and IL-13 showed that IL-13 skewed the macrophage polarization toward M1. The above studies have shown that there is a certain proinflammatory immune response in the pulmonary arteries of IPAH patients, and that IL-13 can inhibit this excessive proinflammatory response to a certain extent.

In summary, IL-13 can mediate the phenotype of PASMC by possibly regulating the expression of the downstream hub genes in the pathogenic process of IPAH. Regulation of the hub genes EWSR1, SNRPB, HNRNPU, HNRNPH1, HNRNPA3 and the 3'UTR sites miR-1-3p/206, miR-383-5p, and miR-155-5p may be the key functions of IL-13, which provides some bioinformatic basis for the molecular diagnosis of IPAH patients and the selection of therapeutic targets. Further studies based on datasets with larger sample size are needed to better understand the mechanism for the regulation of IL-13 on immune response in IPAH.

Acknowledgements

We thank the authors who built the datasets (GSE15739, GSE130391).

Disclosure of conflict of interest

None.

Address correspondence to: Qingshi Zeng, Department of Radiology, The First Affiliated Hospital of Shandong First Medical University & Shandong Provincial Qianfoshan Hospital, No. 16766, Jingshi Road, Lixia District, Jinan 250011, Shandong, P. R. China. Tel: +86-0317-8881120; Fax: +86-0317-8881120; E-mail: zengqingshi@sina.com

References

[1] Galie N, Humbert M, Vachiery JL, Gibbs S, Lang I, Torbicki A, Simonneau G, Peacock A, Vonk Noordegraaf A, Beghetti M, Ghofrani A, Gomez Sanchez MA, Hansmann G, Klepetko W, Lancellotti P, Matucci M, McDonagh T, Pierard LA, Trindade PT, Zompatori M and Hoeper M; ESC Scientific Document Group. 2015 ESC/ERS guidelines for the diagnosis and treatment of

pulmonary hypertension: the joint task force for the diagnosis and treatment of pulmonary hypertension of the European society of cardiology (ESC) and the European respiratory society (ERS); endorsed by: association for European paediatric and congenital cardiology (AEPC), International society for heart and lung transplantation (ISHLT). *Eur Heart J* 2016; 37: 67-119.

- [2] Voelkel NF, Gomez-Arroyo J, Abbate A, Bogaard HJ and Nicolls MR. Pathobiology of pulmonary arterial hypertension and right ventricular failure. *Eur Respir J* 2012; 40: 1555-1565.
- [3] Morrell NW, Aldred MA, Chung WK, Elliott CG, Nichols WC, Soubrier F, Trembath RC and Loyd JE. Genetics and genomics of pulmonary arterial hypertension. *Eur Respir J* 2019; 53: 1801899.
- [4] Jandl K, Marsh LM, Hoffmann J, Mutgan AC, Baum O, Bloch W, Thekkekara-Puthenparampil H, Kolb D, Sinn K, Klepetko W, Heinemann A, Olschewski A, Olschewski H and Kwapiszewska G. Basement membrane remodeling controls endothelial function in idiopathic pulmonary arterial hypertension. *Am J Respir Cell Mol Biol* 2020; 63: 104-117.
- [5] Savai R, Pullamsetti SS, Kolbe J, Bieniek E, Vowinckel R, Fink L, Scheed A, Ritter C, Dahal BK, Vater A, Klussmann S, Ghofrani HA, Weissmann N, Klepetko W, Banat GA, Seeger W, Grimminger F and Schermuly RT. Immune and inflammatory cell involvement in the pathology of idiopathic pulmonary arterial hypertension. *Am J Respir Crit Care Med* 2012; 186: 897-908.
- [6] Shen Q, Chen W, Liu J and Liang QS. Galectin-3 aggravates pulmonary arterial hypertension via immunomodulation in congenital heart disease. *Life Sci* 2019; 232: 116546.
- [7] Soon E, Holmes AM, Treacy CM, Doughty NJ, Southgate L, Machado RD, Trembath RC, Jennings S, Barker L, Nicklin P, Walker C, Budd DC, Pepke-Zaba J and Morrell NW. Elevated levels of inflammatory cytokines predict survival in idiopathic and familial pulmonary arterial hypertension. *Circulation* 2010; 122: 920-927.
- [8] May RD and Fung M. Strategies targeting the IL-4/IL-13 axes in disease. *Cytokine* 2015; 75: 89-116.
- [9] Hecker M, Zaslona Z, Kwapiszewska G, Niess G, Zakrzewicz A, Hergenreider E, Wilhelm J, Marsh LM, Sedding D, Klepetko W, Lohmeyer J, Dimmeler S, Seeger W, Weissmann N, Schermuly RT, Kneidinger N, Eickelberg O and Morty RE. Dysregulation of the IL-13 receptor system: a novel pathomechanism in pulmonary arterial hypertension. *Am J Respir Crit Care Med* 2010; 182: 805-818.

IL-13 is involved in the progression of IPAH

- [10] McCormick SM and Heller NM. Commentary: IL-4 and IL-13 receptors and signaling. *Cytokine* 2015; 75: 38-50.
- [11] Masson B, Montani D, Humbert M, Capuano V and Antigny F. Role of store-operated Ca(2+) entry in the pulmonary vascular remodeling occurring in pulmonary arterial hypertension. *Biomolecules* 2021; 11: 1781.
- [12] Clough E and Barrett T. The gene expression omnibus database. *Methods Mol Biol* 2016; 1418: 93-110.
- [13] Halliday SJ, Matthews DT, Talati MH, Austin ED, Su YR, Absi TS, Fortune NL, Gailani D, Matafonov A, West JD and Hemnes AR. A multifaceted investigation into molecular associations of chronic thromboembolic pulmonary hypertension pathogenesis. *JRSM Cardiovasc Dis* 2020; 9: 2048004020906994.
- [14] Szklarczyk D, Franceschini A, Kuhn M, Simonovic M, Roth A, Minguez P, Doerks T, Stark M, Muller J, Bork P, Jensen LJ and von Mering C. The STRING database in 2011: functional interaction networks of proteins, globally integrated and scored. *Nucleic Acids Res* 2011; 39: D561-568.
- [15] Shannon P, Markiel A, Ozier O, Baliga NS, Wang JT, Ramage D, Amin N, Schwikowski B and Ideker T. Cytoscape: a software environment for integrated models of biomolecular interaction networks. *Genome Res* 2003; 13: 2498-2504.
- [16] Wujak M, Veith C, Wu CY, Wilke T, Kanbagli ZI, Novoyatleva T, Guenther A, Seeger W, Grimminger F, Sommer N, Schermuly RT and Weissmann N. Adenylate kinase 4-A key regulator of proliferation and metabolic shift in human pulmonary arterial smooth muscle cells via Akt and HIF-1 α Signaling pathways. *Int J Mol Sci* 2021; 22: 10371.
- [17] McGeary SE, Lin KS, Shi CY, Pham TM, Bisaria N, Kelley GM and Bartel DP. The biochemical basis of microRNA targeting efficacy. *Science* 2019; 366: eaav1741.
- [18] Huang da W, Sherman BT and Lempicki RA. Systematic and integrative analysis of large gene lists using DAVID bioinformatics resources. *Nat Protoc* 2009; 4: 44-57.
- [19] Uhlen M, Fagerberg L, Hallstrom BM, Lindskog C, Oksvold P, Mardinoglu A, Sivertsson A, Kampf C, Sjostedt E, Asplund A, Olsson I, Edlund K, Lundberg E, Navani S, Szigyanto CA, Odeberg J, Djureinovic D, Takanen JO, Hober S, Alm T, Edqvist PH, Berling H, Tegel H, Mulder J, Rockberg J, Nilsson P, Schwenk JM, Hamsten M, von Feilitzen K, Forsberg M, Persson L, Johansson F, Zwahlen M, von Heijne G, Nielsen J and Ponten F. Proteomics. Tissue-based map of the human proteome. *Science* 2015; 347: 1260419.
- [20] Newman AM, Liu CL, Green MR, Gentles AJ, Feng W, Xu Y, Hoang CD, Diehn M and Alizadeh AA. Robust enumeration of cell subsets from tissue expression profiles. *Nat Methods* 2015; 12: 453-457.
- [21] Hashimoto-Kataoka T, Hosen N, Sonobe T, Arita Y, Yasui T, Masaki T, Minami M, Inagaki T, Miyagawa S, Sawa Y, Murakami M, Kumano-goh A, Yamauchi-Takahara K, Okumura M, Kishimoto T, Komuro I, Shirai M, Sakata Y and Nakaoka Y. Interleukin-6/interleukin-21 signaling axis is critical in the pathogenesis of pulmonary arterial hypertension. *Proc Natl Acad Sci U S A* 2015; 112: E2677-2686.
- [22] Wang YC, Chen S and Du JB. Bosentan for treatment of pediatric idiopathic pulmonary arterial hypertension: state-of-the-art. *Front Pediatr* 2019; 7: 302.
- [23] Liu BX, Zhu LP, Yuan P, Marsboom G, Hong ZG, Liu JM, Zhang P and Hu QH. Comprehensive identification of signaling pathways for idiopathic pulmonary arterial hypertension. *Am J Physiol Cell Physiol* 2020; 318: C913-C930.
- [24] Elinoff JM, Mazer AJ, Cai R, Lu M, Graninger G, Harper B, Ferreyra GA, Sun J, Solomon MA and Danner RL. Meta-analysis of blood genome-wide expression profiling studies in pulmonary arterial hypertension. *Am J Physiol Lung Cell Mol Physiol* 2020; 318: L98-L111.
- [25] Bieber T. Interleukin-13: targeting an underestimated cytokine in atopic dermatitis. *Allergy* 2020; 75: 54-62.
- [26] Orihuela R, McPherson CA and Harry GJ. Microglial M1/M2 polarization and metabolic states. *Br J Pharmacol* 2016; 173: 649-665.
- [27] Xin Y, Tang L, Chen J, Chen D, Wen W and Han FG. Inhibition of miR1013p protects against sepsis-induced myocardial injury by inhibiting MAPK and NF κ B pathway activation via the upregulation of DUSP1. *Int J Mol Med* 2021; 47: 20.
- [28] Chen QL, Li XY, Kong LJ, Xu Q, Wang Z and Lv QZ. miR-101-3p induces vascular endothelial cell dysfunction by targeting tet methylcytosine dioxygenase 2. *Acta Biochim Biophys Sin (Shanghai)* 2020; 52: 180-191.
- [29] Yao DH, Zhou ZY, Wang PF, Zheng L, Huang YH, Duan YT, Liu B and Li YS. MiR-125-5p/IL-6R axis regulates macrophage inflammatory response and intestinal epithelial cell apoptosis in ulcerative colitis through JAK1/STAT3 and NF- κ B pathway. *Cell Cycle* 2021; 20: 2547-2564.
- [30] Zhong YY and Luo LY. Exosomes from human umbilical vein endothelial cells ameliorate ischemic injuries by suppressing the rna component of mitochondrial rna-processing endoribonuclease via the induction of miR-206/

IL-13 is involved in the progression of IPAH

- miR-1-3p levels. *Neuroscience* 2021; 476: 34-44.
- [31] Huang SS, Ding DF, Chen S, Dong CL, Ye XL, Yuan YG, Feng YM, You N, Xu JR, Miao H, You Q, Lu X and Lu YB. Resveratrol protects podocytes against apoptosis via stimulation of autophagy in a mouse model of diabetic nephropathy. *Sci Rep* 2017; 7: 45692.
- [32] Takuma A, Abe A, Saito Y, Nito C, Ueda M, Ishimaru Y, Harada H, Abe K, Kimura K and Asakura T. Gene expression analysis of the effect of ischemic infarction in whole blood. *Int J Mol Sci* 2017; 18: 2335.
- [33] Li GS, Cui L and Wang GD. miR-155-5p regulates macrophage M1 polarization and apoptosis in the synovial fluid of patients with knee osteoarthritis. *Exp Ther Med* 2021; 21: 68.
- [34] Shi YJ, Fu XL, Cao Q, Mao ZD, Chen Y, Sun Y, Liu ZG and Zhang Q. Overexpression of miR-155-5p inhibits the proliferation and migration of IL-13-induced human bronchial smooth muscle cells by suppressing TGF-beta-activated kinase 1/MAP3K7-binding protein 2. *Allergy Asthma Immunol Res* 2018; 10: 260-267.
- [35] Chen L, Zheng SY, Yang CQ, Ma BM and Jiang D. MiR-155-5p inhibits the proliferation and migration of VSMCs and HUVECs in atherosclerosis by targeting AKT1. *Eur Rev Med Pharmacol Sci* 2019; 23: 2223-2233.
- [36] Geuens T, Bouhy D and Timmerman V. The hnRNP family: insights into their role in health and disease. *Hum Genet* 2016; 135: 851-867.
- [37] Wang L, Wen MY and Cao XT. Nuclear hnRNP-A2B1 initiates and amplifies the innate immune response to DNA viruses. *Science* 2019; 365: eaav0758.
- [38] Gal Z, Gezsi A, Semsei AF, Nagy A, Sultesz M, Csoma Z, Tamasi L, Galfy G and Szalai C. Investigation of circulating lncRNAs as potential biomarkers in chronic respiratory diseases. *J Transl Med* 2020; 18: 422.
- [39] Li JS, Zhao P, Tian YG, Li KC, Zhang LX, Guan QZ, Mei XF and Qin YQ. The Anti-inflammatory effect of a combination of five compounds from five chinese herbal medicines used in the treatment of COPD. *Front Pharmacol* 2021; 12: 709702.
- [40] Nishida Y, Aida K, Kihara M and Kobayashi T. Antibody-validated proteins in inflamed islets of fulminant type 1 diabetes profiled by laser-capture microdissection followed by mass spectrometry. *PLoS One* 2014; 9: e107664.
- [41] Comegna M, Succoio M, Napolitano M, Vitale M, D'Ambrosio C, Scaloni A, Passaro F, Zambano N, Cimino F and Faraonio R. Identification of miR-494 direct targets involved in senescence of human diploid fibroblasts. *FASEB J* 2014; 28: 3720-3733.
- [42] Lee J, Nguyen PT, Shim HS, Hyeon SJ, Im H, Choi MH, Chung S, Kowall NW, Lee SB and Ryu H. EWSR1, a multifunctional protein, regulates cellular function and aging via genetic and epigenetic pathways. *Biochim Biophys Acta Mol Basis Dis* 2019; 1865: 1938-1945.
- [43] Beers DR and Appel SH. Immune dysregulation in amyotrophic lateral sclerosis: mechanisms and emerging therapies. *Lancet Neurol* 2019; 18: 211-220.
- [44] Wang H, Demirkan G, Bian X, Wallstrom G, Barker K, Karthikeyan K, Tang Y, Pasha SF, Leighton JA, Qiu J and LaBaer J. Identification of antibody against SNRPB, small nuclear Ribonucleoprotein-associated proteins B and B', as an autoantibody marker in Crohn's disease using an immunoproteomics approach. *J Crohns Colitis* 2017; 11: 848-856.
- [45] Xie N, Chen M, Dai RL, Zhang Y, Zhao HQ, Song ZM, Zhang LF, Li ZY, Feng YQ, Gao H, Wang L, Zhang T, Xiao RP, Wu JX and Cao CM. SRSF1 promotes vascular smooth muscle cell proliferation through a Delta133p53/EGR1/KLF5 pathway. *Nat Commun* 2017; 8: 16016.
- [46] Xu J, Yang YC, Yang YJ and Xiong CM. Identification of potential risk genes and the immune landscape of idiopathic pulmonary arterial hypertension via microarray gene expression dataset reanalysis. *Genes (Basel)* 2021; 12: 125.